doi:10.1093/brain/awn111 *Brain* (2008), **131**, 1818–1830

Epileptogenicity of brain structures in human temporal lobe epilepsy: a quantified study from intracerebral EEG

Fabrice Bartolomei,[1,2,3] Patrick Chauvel[1,2,3] and Fabrice Wendling[4,5]

[1]INSERM, U751, Marseille, F-13000, [2]Aix Marseille Université, Faculté de Médecine, Marseille, F-13000, [3]Assistance Publique – Hôpitaux de Marseille, Hôpital de la Timone, Service de Neurophysiologie Clinique, Marseille, F-13000, [4]INSERM, U642, Rennes, F-35000 and [5]Université de Rennes I, LTSI, Rennes, F-35000, France

Correspondence to: Fabrice Bartolomei, Hôpital de la Timone, Service de Neurophysiologie Clinique, 264 Rue Saint-Pierre, Marseille 13005, France
E-mail: fabrice.bartolomei@ap-hm.fr

The identification of brain regions generating seizures ('epileptogenic zone', EZ) in patients with refractory partial epilepsy is crucial prior to surgery. During pre-surgical evaluation, this identification can be performed from the analysis of intracerebral EEG. In particular, the presence of high-frequency oscillations, often referred to as 'rapid discharges', has long been recognized as a characteristic electrophysiological pattern of the EZ. However, to date, there has been no attempt to make use of this specific pattern to quantitatively evaluate the degree of epileptogenicity in recorded structures. A novel quantitative measure that characterizes the epileptogenicity of brain structures recorded with depth electrodes is presented. This measure, called 'Epileptogenicity Index' (EI), is based on both spectral (appearance of fast oscillations replacing the background activity) and temporal (delay of appearance with respect to seizure onset) properties of intracerebral EEG signals. EI values were computed in mesial and lateral structures of the temporal lobe in a group of 17 patients with mesial temporal lobe epilepsy (MTLE). Statistically high EI values corresponded to structures involved early in the ictal process and producing rapid discharges at seizure onset. In all patients, these high values were obtained in more than one structure of the temporal lobe region. In the majority of patients, highest EI values were computed from signals recorded in mesial structures. In addition, when averaged over patients, EI values gradually decreased from structure to structure. For lateral neocortex, higher EI values were found in patients with normal MRI, in contrast with patients with hippocampal sclerosis. In this former sub-group of patients, a greater number of epileptogenic structures was also found. A statistically significant correlation was found between the duration of epilepsy and the number of structures disclosing high epileptogenicity suggesting that MTLE is a gradually evolving process in which the epileptogenicity of the temporal lobe tends to increase with time.

Keywords: partial epilepsy; high-frequency oscillations; epileptogenic zone; seizure onset

Abbreviations: EC = entorhinal cortex; EI = epileptogenicity index; EZ = epileptogenic zone; HS = hippocampal sclerosis; MRI = magnetic resonance imaging; MTLE = mesial temporal lobe epilepsy; STG = superior temporal gyrus

Received January 20, 2008. Revised April 3, 2008. Accepted May 12, 2008. Advance Access publication June 13, 2008

Introduction

Over the past decades, a sustained research effort has been undertaken to localize and to characterize the cerebral areas involved in the genesis and the propagation of focal epileptic seizures. Indeed, the identification of the so-called 'epileptogenic zone' (EZ) (Bancaud *et al.*, 1965), usually defined as the subset of brain sites involved in the generation of seizures, is crucial in the context of epilepsy surgery as the aim of the surgical procedure is precisely to remove the EZ.

The non-negligible rate of failure in epilepsy surgery brings evidence that the question of the definition of the epileptogenic zone is still unsolved and that progress must still be made in order to determine the epileptogenicity of the brain regions in a patient-specific context.

One puzzling feature is that brain activity at seizure onset may disclose complex electrophysiological patterns, often with the involvement of several distinct structures.

Therefore, in a large number of cases, this typical observation shows that the EZ can hardly be described as

a simple epileptic focus (Bartolomei *et al.*, 2001*a*, 2005; Spencer, 2002).

For clinicians facing the problem of the definition of the EZ from the analysis of intracerebral EEG signals, two parameters are generally considered in order to qualitatively determine the degree of 'epileptogenicity' of a given structure and its subsequent contribution to the EZ. The first parameter is the capability of a given structure to generate high-frequency oscillations, typically in the beta or/and the gamma range. These oscillations are classically referred to as 'rapid discharges' (Allen *et al.*, 1992; Alarcon *et al.*, 1995; Wendling *et al.*, 2003). Rapid discharges have been long recognized to be one of the most characteristic patterns of the EZ in focal epilepsy (Bancaud *et al.*, 1965). The surgical prognosis has also been found to be related to the removal of regions with rapid discharges (Alarcon *et al.*, 1995).

The second parameter is the delay of involvement of the structure with respect to the onset of the seizure. Indeed, it is generally accepted that the earlier the appearance of a rapid discharge in a given brain area, the more epileptogenic this area.

Therefore, both the spectral content and the delay of appearance of the fast ictal activity appear as crucial parameters for determining the EZ. However, no attempt to quantify the combination of these two phenomena (appearance of high-frequency oscillations and latency with respect to seizure onset time) has been made. Consequently, there exists no strict quantitative criterion to define the EZ.

In the present study, we propose a new approach to quantify the 'epileptogenicity' of recorded brain structures from on the analysis of intracerebral EEG signals. This approach is based on an 'Epileptogenicity Index' (EI) that combines both spectral and temporal parameters, respectively related to the propensity of a brain area to generate rapid discharges and to the time for this area to become involved into the seizure process.

We chose to first develop and validate this approach in the context of mesial temporal lobe epilepsies (MTLE), considered to be a well-known model of 'multistructural' epileptogenic zone (Bragin *et al.*, 2000; Bartolomei *et al.*, 2004*b*). Indeed, it is quite usual that distinct structures of the mesial part of the temporal lobe are conjointly involved at the beginning of seizures. The participation of the hippocampus, as well as that of the amygdala to a lesser extent, has been reported in a number of studies and is now well known (Wieser, 1983). More recently, it has been shown that other mesial temporal lobe structures may also play a key role in seizure genesis, such as the entorhinal cortex (EC) (Spencer and Spencer, 1994; Bartolomei *et al.*, 2005) or the limbic part of the temporal pole (Chabardes *et al.*, 1999). It has also been proposed that the EZ in MTLE is organized as a network of several epileptogenic structures instead of a single 'monostructural' focus (Bragin *et al.*, 2000; Bartolomei *et al.*, 2004*b*; Briellmann *et al.*, 2004).

In the present study, the epileptogenicity index was computed in mesial and lateral structures of the temporal lobe in patients with MTLE.

Two types of MTLE were included, one with hippocampal sclerosis (HS) and the other with normal MRI [the so-called 'paradoxical MTLE' (Cohen-Gadol *et al.*, 2005)]. We indeed used this quantification to examine the possibility that epileptogenic networks could differ according to the underlying pathology. We also sought to determine the relationship between the extent of the EZ (in term of regions exhibiting high EI values) with the epilepsy duration in this group of patients.

Methods

Patient selection and SEEG recording

Seventeen patients undergoing pre-surgical evaluation of drug-resistant TLE were selected from a series of 130 patients in whom intracerebral recordings had been performed since 2000.

All patients had a comprehensive evaluation including detailed history and neurological examination, neuropsychological testing, routine magnetic resonance imaging (MRI), surface electroencephalography (EEG) and stereoelectroencephalography (SEEG, depth electrodes). Patients were selected for the present study if they satisfied the following criteria: (i) seizures involved the mesial temporal lobe at onset; (ii) MRI was either normal or disclosed patterns suggestive of HS (hippocampal atrophy and hyperintensity on flair sequences).

SEEG exploration was carried out during long-term video-EEG monitoring. Recordings were performed using intracerebral multiple contact electrodes (10–15 contacts, length: 2 mm, diameter: 0.8 mm, 1.5 mm apart) placed according to Talairach's stereotactic method (Bancaud *et al.*, 1970; Talairach *et al.*, 1992), as illustrated in Fig. 1.

The anatomical targeting of electrodes was established in each patient according to available non-invasive information and hypotheses about the localization of the epileptogenic zone. A preplanning of the implantation was performed on 3D T1 MRI images using a dedicated software ('Brainvisa', http://brainvisa.info) for surface rendering calculation, cortical anatomy analysis and sulci labelling (Mangin *et al.*, 2004; Regis *et al.*, 2005). The final definition of each electrode trajectory was elaborated on a workstation allowing for stereotactic registration of preoperative stereotactic MR and preoperative stereotactic telemetric angiography. A post-operative computerized tomography (CT) scan without contrast was then used to verify the absence of bleeding and the position of electrodes. Video-EEG recording was prolonged as long as necessary in order to record several of the patient's habitual seizures. Intracerebral electrodes were then removed and an MRI performed, permitting visualization of the trajectory of each electrode (3DT_1-weighted images and T_2-weighted coronal images, siemens 1.5T). Finally, CT-scan/MRI data fusion was performed to accurately check the anatomical location of each contact along the electrode trajectory according to previously described procedures (Bartolomei *et al.*, 2004*a*). In the 17 selected patients, several distinct functional regions of the temporal lobe were explored via an orthogonal implantation of depth electrodes (Maillard *et al.*, 2004). All patients had electrodes that spatially sampled mesial/limbic regions including amygdala (AMY), EC, internal part of the

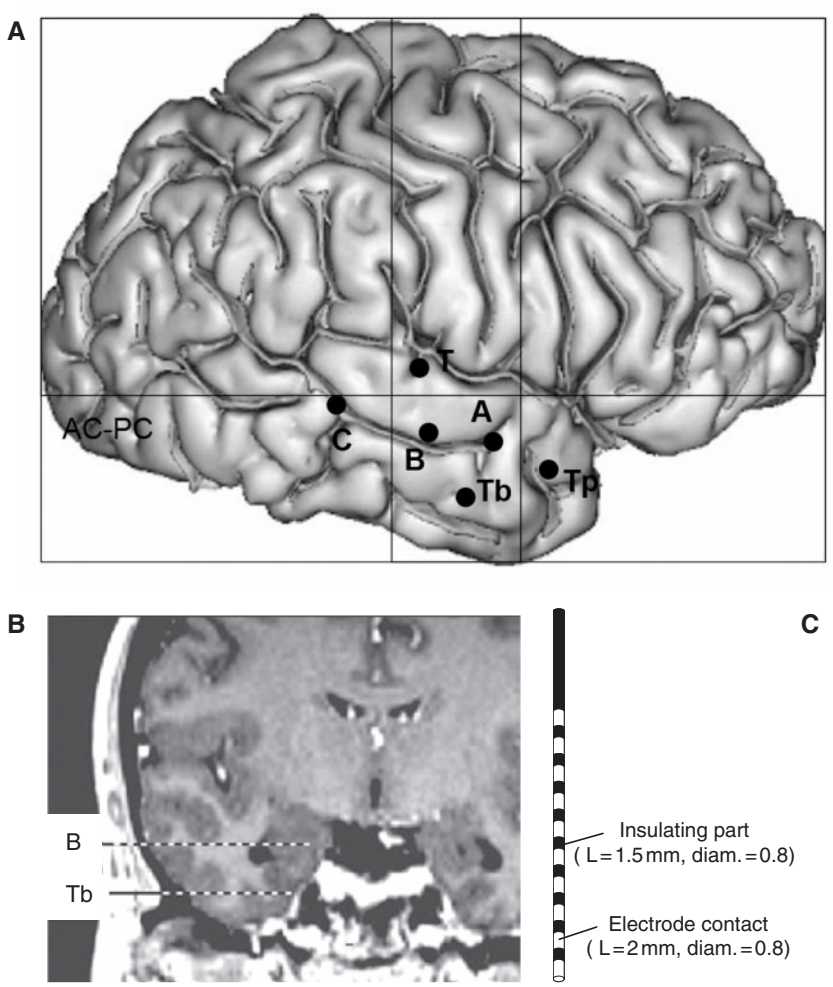

Fig. 1 Example of depth electrodes implantation for stereoelectroencephalographic (SEEG) exploration in temporal lobe epilepsy (patient P4) (**A**) Lateral view of all depth electrodes superimposed on a 3D reconstruction of the neocortical surface of the brain. In this case, brain structures are explored with six intracerebral multiple contact electrodes denoted by letters A, B, C, Tp, Tb, T. Internal contacts of electrodes Tp, A, B, and C record four mesial structures (resp. the internal part of the temporal pole, the amygdala, the anterior hippocampus, and the posterior hippocampus) while external contacts record four lateral structures (resp. the external part of the temporal pole, the anterior, the middle and the posterior part of MTG). Internal and external contacts of electrode T explore two main structures (resp. the insula and the superior temporal gyrus). Internal contacts of electrode Tb reaches the entorhinal cortex. (**B**) Reconstruction of the trajectory of the electrodes Tb and B superimposed on the coronal MRI view. (**C**) Schematic diagram of the electrodes used in SEEG exploration (L = length, diam = diameter).

temporal pole (iTp), the anterior part of the hippocampus (HiA), the posterior part of the hippocampus (HiP) and lateral/neocortical regions of temporal lobe. Most of the patients also had electrodes exploring extratemporal regions (prefrontal lobe and parietal cortex) in order to determine seizure propagation pathways or alternative hypothesis.

Signals were recorded on a 128 channel Deltamed^{TM} system. They were sampled at 256 Hz and recorded on a hard disk (16 bits/sample) using no digital filter. Two hardware filters were present in the acquisition procedure. The first is a high-pass filter (cut-off frequency equal to 0.16 Hz at –3 dB) used to remove very slow variations that sometimes contaminate the baseline. The second is a first-order low-pass filter (cut-off frequency equal to 97 Hz at –3 dB) to avoid aliasing. Table 1 provides clinical information about the patients selected for the purpose of this study.

SEEG signal analysis: computation of the EI

High-frequency oscillations are frequently observed during the transition from interictal to ictal activity. They are often referred to as 'rapid discharges' as they constitute a typical electrophysiological pattern characterized by a noticeable increase of signal frequency. Classically, the rapid discharge is a transient phenomenon, which lasts for a few seconds and which may or may not be associated with voltage reduction.

In order to characterize both the propensity of a given brain structure to a rapid discharge and the delay of appearance of this discharge with respect to seizure onset, we introduce a new index referred to as the 'Epileptogenicity Index'.

The purpose of this index is to provide quantified information about the behaviour of recorded brain structures from signals they generate during the seizure process (from onset to termination).

This index summarizes two pieces of information into a single quantity: (i) whether or not the recorded brain structure is involved in the generation of a rapid discharge and (ii) when involved, whether or not this rapid discharge is delayed with respect to rapid discharges generated by other structures.

Therefore, from the methodological point of view, computation of the 'Epileptogenicity Index' requires a preliminary step aimed at detecting rapid discharges in SEEG signals during transition to seizure, as described later.

Detection of rapid discharges

The detection of abrupt changes in a random signal is a classical but difficult problem in signal processing (Basseville and Nikiforov, 1993). Optimal solution to this problem consists in (i) building a statistic (i.e. a 'marker') that characterizes the changes to be detected in the signal and (ii) by applying a procedure on this quantity aimed at estimating the time instants at which changes occur, as accurately as possible.

In our case, the specific change to be detected in the signal is the appearance of a fast oscillation, the frequency of which typically belongs to the EEG high-beta or low-gamma band in mesial temporal lobe seizures (Spencer *et al.*, 1992; Bartolomei *et al.*, 2004*b*).

Consequently, we designed a two-stage procedure based on the signal energy distribution in the spectral domain (step 1) and on the use of an optimal algorithm for detecting changes in this distribution (step 2).

Step 1: definition of a statistic that abruptly increases as fast oscillations appear in the signal

Let $x(t)$ denote a monochannel SEEG signal recorded during the transition from interictal to ictal activity. As $x(t)$ is a finite-energy signal, its energy spectral density $\Gamma(w)$ is the square of the magnitude of its Fourier transform $X(w)$:

$$\Gamma(w) = \frac{X(w)X^*(w)}{2\pi}$$

$\Gamma(w)$ describes how the energy of signal $x(t)$ is distributed in frequency. The integral of $\Gamma(w)$ over a frequency interval $[w_1, w_2]$ provides the energy of $x(t)$ in the frequency sub-band ranging from w_1 to w_2.

Let θ, α, β and γ denote the frequency sub-bands classically used to categorize rhythms reflected by EEG signals.

From $\Gamma(w)$ and from these sub-bands, we defined a quantity, denoted as ER, corresponding to the signal energy ratio between high (β, γ) and low (θ, α) frequency bands of the EEG:

$\mathrm{ER} = (E_\beta + E_\gamma)/(E_\theta + E_\alpha)$ where $E_{\text{sub-band}} = \int_{\text{sub-band}} \Gamma(w)\,dw$ and where sub-band denotes θ, α, β and γ frequency sub-bands (see Table 2 for boundary values of each sub-band).

In practice, $x(t)$ is a discrete time-series (digitized EEG) denoted by $x[n]$, $n = k \times \Delta T$, $k = 0, 1, \ldots, N$ where ΔT is the sampling period. $\Gamma(w)$ is estimated over a sliding window of duration D using the periodogram method (i.e. averaging of discrete spectra obtained from the Fast Fourier Transform of $x[n]$). Therefore, the obtained statistic $\mathrm{ER}[n]$ is time-varying.

Step 2: optimal detection of rapid discharges

$\mathrm{ER}[n]$ is sensitive to frequency changes in the signal. In particular, $\mathrm{ER}[n]$ increases when θ–α activity (that is predominant in background SEEG signals) changes into β–γ activity (that is predominant in SEEG signals during rapid discharges). Conversely, as the β–γ activity vanishes (at the end of the fast onset activity and as slower theta rhythms appear in the seizure), $\mathrm{ER}[n]$ is expected to drop down. Therefore, these physiological changes observed in SEEG signal frequency are reflected by the mean value (over time) of statistic $\mathrm{ER}[n]$. An example is provided in Fig. 2 which shows the behaviour of $\mathrm{ER}[n]$ on the intracerebral SEEG signal recorded from the EC (Fig. 2A) during the transition from interictal to seizure activity. As depicted in Fig. 2B, $\mathrm{ER}[n]$ dramatically increases at seizure onset, stays high during the rapid discharge and then decreases as the signal frequency gradually slows down during the ictal phase.

An optimal algorithm for detecting change-points in a random quantity was proposed by Page (1954) and Hinkley (1970). The key idea of this algorithm (also known as the 'cumulative sum algorithm' or 'CUSUM') is to perform a test on the mean of the quantity to analyse (in our case, the statistic $\mathrm{ER}[n]$).

Table 1 Main clinical features of the 17 studied patients (P1–P17)

Patient	Gender	Epilepsy duration (years)	Age at seizure onset (years)	Surgical outcome	MRI	Side	$N_{IE \geq 0.3}$
P1	F	32	3	IIA	HS	R	5(4)
P2	F	37	8	IA	HS	L	5(5)
P3	F	30	3	IB	N	L	5(4)
P4	M	15	14	IA	HS	R	3(3)
P5	F	11	3	IA	HS	L	2(2)
P6	M	20	10	IA	HS	R	3(3)
P7	F	28	2	IIA	HS	L	3(3)
P8	F	20	10	IA	HS	L	2(2)
P9	M	12	5	IA	HS	L	4(4)
P10	M	29	3	IA	HS	R	4(4)
P11	F	20	16	IA	HS	R	3(3)
P12	F	13	25	IA	HS	L	2(2)
P13	M	18	4	IIA	HS	R	4(3)
P14	M	18	18	NO	N	L	6
P15	M	15	17	IIB	HS	L	1(1)
P16	M	28	14	IIA	N	R	6(5)
P17	F	34	28	III	N	L	6(4)

N = normal MRI, $N_{IE \geq 0.3}$ = number of brain structures disclosing an epileptogenicity index value greater than 0.3. In brackets is indicated an estimation of the number of structures disclosing $N_{IE \geq 0.3}$ and surgically removed. Surgical outcome refers to the Engel's classification (follow up duration >2 years for all the patients), NO = not operated.

Table 2 Lower and upper values of frequency bands used in this study (Adapted from (Niedermeyer and Lopes Da Silva, 1999)

Frequency band	Range (Hz)
θ (Theta)	$3.5 \leqslant f < 7.4$
α (Alpha)	$7.4 \leqslant f < 12.4$
β (Beta)	$12.4 \leqslant f < 24$
γ (Gamma)	$24 \leqslant f < 97$[a]

[a]Signals were sampled at 256 Hz.
The theoretical maximum frequency value of 128 Hz is reduced due to the anti-aliasing low-pass filter of the recording system which has a cut-off frequency equal to 97 Hz.

To proceed, a variable denoted by U_N is introduced. Formally, U_N is defined as the difference, cumulated up to step N, between the ER$[n]$ and their average ER$_n$, minus a positive bias v:

$$\mathrm{ER}_n = \frac{1}{n}\sum_{k=1}^{n}\mathrm{ER}[k]$$

$$U_N = \sum_{n=1}^{N}(\mathrm{ER}[n] - \mathrm{ER}_n - v)$$

By construction, U_N is a monotonically decreasing function under the null hypothesis (H0: no change has occurred in ER$[n]$). As a rise occurs in the mean value of ER$[n]$, U_N first exhibits a local minimum u_N and then starts to increase. The decision that this change occurring in ER$[n]$ is significant is taken when $U_N - u_N$ reaches a threshold λ:

$$u_N = \min(U_n, n = 1 \ldots N)$$

H0 is rejected when $(U_N - u_N) > \lambda$

After detection, the algorithm is re-initialized ($U_N = 0$, $u_N = 0$). It is noteworthy that this algorithm provides two quantities of interest when a change occurs in the analysed statistic: (i) the alarm time (N_a)

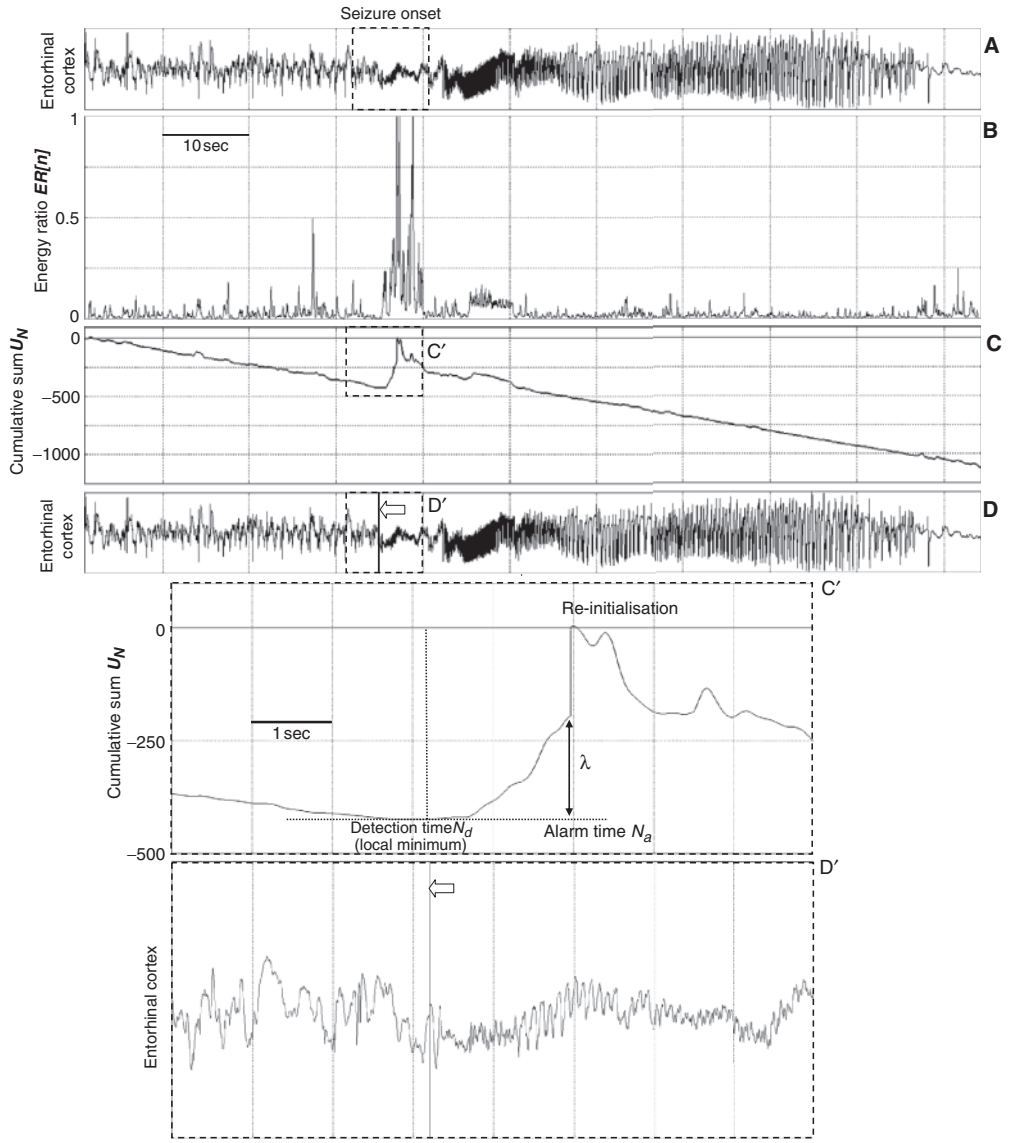

Fig. 2 Signal-processing method developed for estimating the initial time of rapid discharges occurring at the onset of TLE seizures. (**A**) Depth-EEG signal recorded from the entorhinal cortex during the transition from interictal to ictal activity. The method is based on the definition of a statistic (ER: ratio of signal energy in high and low-frequency bands) that abruptly increases as fast oscillations appear in the signal (**B**) and on the application of the Page–Hinkley algorithm on this statistic (**C**). The key idea of the Page–Hinkley algorithm is to perform a test on the mean of ER statistic by building a quantity (cumulative sum U_N) that monotonically decreases when there is no change in the signal and that reaches a local minimum when fast oscillations appear. (**C**) Behaviour of the cumulative sum U_N at the onset of the fast ictal discharge and (**D**) automatically estimated detection time (arrow). (**C′**) Magnified view of the cumulative sum U_N as the rapid discharge appears. Decision that a significant change has occurred is taken at alarm time N_a when the increase of the cumulative sum U_N from the last local minimum (providing the detection time N_d) is greater than threshold λ. (**D′**) Magnified view of the depth-EEG signal with the automatically determined marker of the onset of the rapid ictal discharge.

when threshold λ is reached and (ii) the change-point detection time (N_d) corresponding to the last local minimum of U_N. Moreover, in the Page–Hinkley algorithm, results depend on the two aforementioned parameters, namely the value ν of the bias used to compute U_N and the threshold value λ to decide if a significant change has occurred. These parameters are used to adjust the compromise between sensitivity and specificity, as in any detection problem. Parameter ν corresponds to the magnitude of changes that should not raise an alarm. Parameter λ depends on the desired false-alarm rate. The increase of λ reduces the rate of false alarms but also leads to non-detections. In this study, both parameters were defined by the epileptologist using a user-friendly interface that graphically represents estimated detection times upon SEEG signals as the operator is manually adjusting parameter values.

The performance of the algorithm is exemplified in Fig. 2C which shows the evolution of $U[n]$ as a function of time when computed on the intracerebral SEEG signal recorded from the EC during the transition to seizure. The detection time, automatically determined by the algorithm, is shown in Fig. 2D. In order to enhance visual analysis, a zoom is also provided in Fig. 2C′ ($U[n]$) and 2D' (SEEG signal). The result shows that the detection time corresponds to the appearance of the early fast oscillations in the SEEG signal, as expected.

Definition and computation of the EI

The Page–Hinkley algorithm provides a detection time for each brain structure if involved in the generation of a rapid discharge. In order to take into account the time instants at which rapid discharges occur during the seizure process, we arbitrarily define the first detection time as the reference time N_0, as displayed in Fig. 3. Then, for each EEG signal s_i recorded from brain structure S_i, we define the Epileptogenicity Index EI_i as the energy ratio averaged over time just after detection of the rapid discharge in

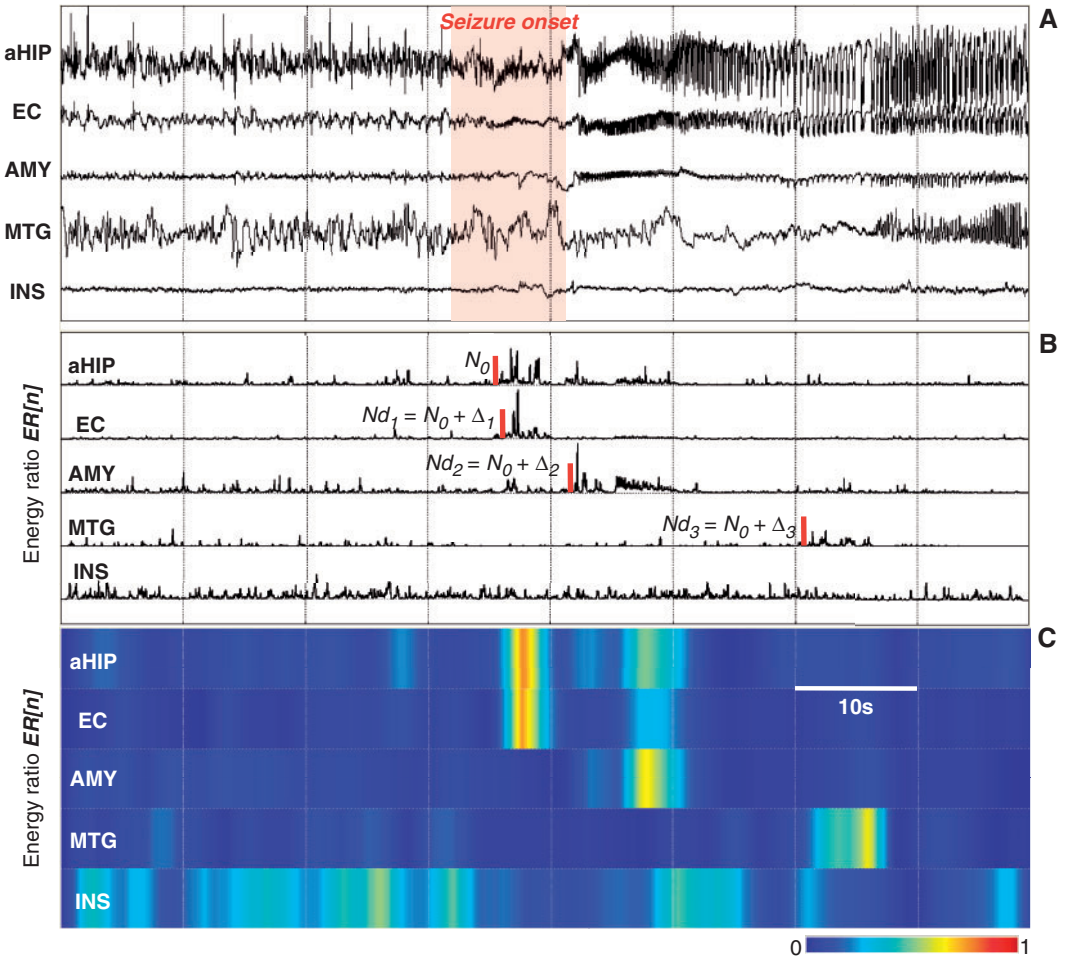

Fig. 3 Delay of involvement of brain structures in the ictal process. (**A**) Example of intracerebral EEG recording (limited to five channels, Patient P2). (**B**) The Page–Hinkley algorithm provides a detection time Nd_1 (red marks) for each brain structure if involved in the generation of a rapid discharge. The first detection time is arbitrarily defined as the reference time N_0 (aHIP in this case). Then, for each EEG signal recorded from a given brain structure (EC, AMY, ...), the Epileptogenicity Index EI is defined as the energy ratio ER[n] (time interval following detection) divided by the delay Δi of involvement of the considered structure with respect to time N_0. (**C**) Colour-coded map showing the evolution of the energy ratio with time (same information as that contained in B). From top to bottom, this representation displays the early involvement of the anterior hippocampus (aHIP) and the entorhinal cortex (EC) as well as the delayed rapid discharge in the amygdala (AMY) and then in the middle temporal gyrus (MTG). Note that the algorithm does not detect any rapid discharge in the insula (INS).

signal s_i and divided by the delay Δi of involvement of structure S_i with respect to time N_0:

$$EI_i = \frac{1}{N_{di} - N_0 + \tau} \sum_{n=N_{di}}^{N_{di}+H} ER[n],\ \tau > 0$$

where N_{di} is the detection time in signal s_i recorded from structure S_i and H is the duration over which ER$[n]$ is integrated. From this equation, it can be observed that the sooner structure S_i gets involved in the seizure, the higher the index EI_i.

Parameter τ accounts for the particular where S_i is the first structure that generates the fast activity ($N_{di} = N_0$) and avoids division by zero. It was arbitrarily set to 1. Another particular case is when structure S_i does not generate fast activity. In this case, N_{di} was set to be equal to the time corresponding to seizure termination. This operation leads to very low value of EI_i, as expected. As the average duration of rapid discharges detected in all patients was $10\,s \pm 6$, parameter H was set to be equal to 5 s.

Finally, in order to end with a normalized value ranging from 0 (no epileptogenicity) to 1 (maximal epileptogenicity) for considered structures S_i, EI_i values were divided by the maximal value obtained in each patient. In the sequel, normalized EI_i values are simply denoted by 'EI values'.

Statistical analysis

A statistical analysis was performed to assess potential links between (i) epileptogenicity and anatomical location of considered structures, (ii) epileptogenicity and presence/absence of HS and (iii) epileptogenicity and patient's history (epilepsy duration).

Therefore, EI values were averaged over two subgroups of structures (located either in the mesial region or the lateral region of the temporal lobe). They were then compared using a Wilcoxon test, which is a non-parametric alternative to the paired Student's *t*-test that does not require assumptions about the statistical distribution of measured values.

EI values computed from the different studied regions were also compared between the two groups of patients with normal MRI and with HS using non-parametric Mann–Whitney test. Finally, a Spearman's rank correlation coefficient was calculated to find possible correlations between the number of significantly high EI values (i.e. >0.3) and the patient age at epilepsy onset or his/her epilepsy duration. All statistical tests were performed on EI values estimated and averaged from three seizures in each patient. A *P*-value $\leqslant 0.05$ was considered to be statistically significant.

Results

Estimation of EI values from mesial and lateral structures

EI were calculated from mesial temporal lobe structures (amygdala, hippocampus, EC and mesial temporal pole) as well as from some lateral cortices (lateral temporal pole, middle and superior temporal gyri and insular cortex). The detailed list of explored brain structures is given in Table 3 along with anatomical location and abbreviated names that are used in Figs 4–7.

Major differences appeared between EI values computed from mesial and lateral cortices in this series of 17 patients (P1–P17) suspected to have MTLE. This result is illustrated in Fig. 4A, which provides the histogram of EI values averaged over patients for the two groups of mesial structures (left column) and lateral structures (right column). It shows that the proposed index clearly distinguished between epileptogenic and non- (or less) epileptogenic structures, as values obtained from lateral structures (0.14 ± 0.17) were found to be significantly ($P = 0.001$) lower than those obtained from mesial structures (0.51 ± 0.15).

Figure 4B represents the EI values averaged over the two groups of mesial and lateral structures for each patient. This figure clearly shows that there is almost no overlap between EI values computed from mesial and lateral structures. This means that all patients have higher EI values when computed from mesial than from lateral structures. The only exception is patient number 17 (P17). In this case, seizures apparently started simultaneously from mesial and lateral cortex and lateral structures appeared to be more epileptogenic than the mesial ones after signal analysis, a feature not suspected from visual analysis of SEEG traces. From the figure, it can also be depicted that the best separation between the two sets of EI values is given by the line EI = 0.3 (dotted line in Fig. 3B). Indeed, all EI values but one (P17) estimated from mesial structures are >0.3. Correspondingly, all EI values but two (P17 and P3) are lower than this threshold value. Figure 4C shows the mean and the standard deviation of IE values obtained from the explored brain regions. In this case, IE values were averaged over the patients. Two main comments can be

Table 3 Brain structures explored with intracerebral electrodes, abbreviated names and location in the temporal lobe region

Brain structure	Abbreviated name	Anatomical location in the temporal lobe
Amygdala	AMY	Mesial
Anterior part of the hippocampus	aHIP	Mesial
Posterior part of the hippocampus	pHIP	Mesial
Entorhinal cortex	EC	Mesial
Internal part of the temporal pole	iTP	Mesial
External part of the temporal pole	eTP	Lateral
Anterior part of the middle temporal gyrus	aMTG	Lateral
Posterior part of the middle temporal gyrus	pMTG	Lateral
Superior temporal gyrus	STG	Lateral
Temporal insular cortex	INS	Lateral

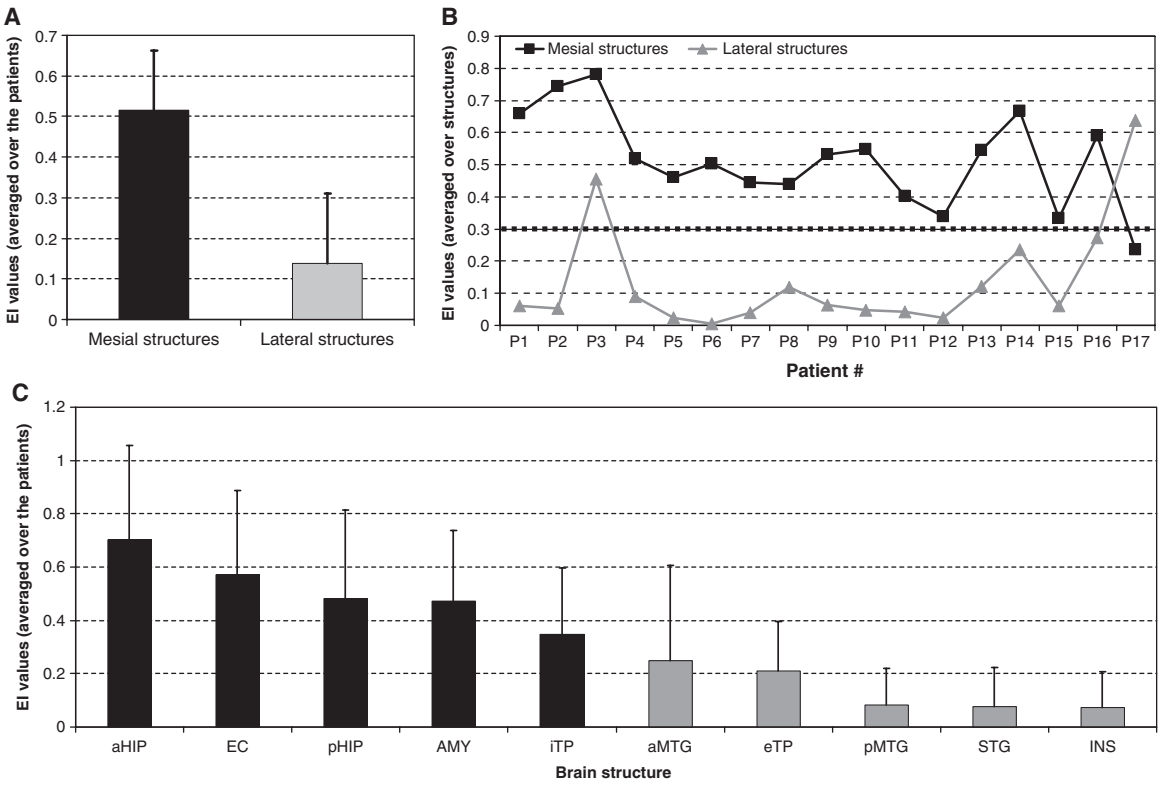

Fig. 4 Values of the Epileptogenicity Index (EI) computed from mesial and lateral structures of the temporal lobe in I7 patients (PI–PI7) with MTLE. (**A**) EI values are averaged over the I7 patients. Mean EI values are significantly higher in mesial (EI averaged from the mesial structures) than lateral structures (EI averaged from the lateral structures) (**B**) The two curves show the values of averaged EI respectively from Mesial structures ((M) and from Lateral structures (L) in the I7 patients. Most of the EI values are above 0.3 for mesial structures and below 0.3 for lateral cortices (**C**) Mean and standard deviation of IE values obtained from the different explored brain regions averaged over the I7 patients for each structure. Black columns: mesial structures. Grey columns: lateral structures. aHIP = anterior hippocampus; EC = entorhinal cortex; pHIP = posterior hippocampus; AMY = amygdale; iTP = internal temporal pole; aMTG = anterior middle temporal gyrus; eTP = external temporal pole; pMTG = posterior part of the middle temporal gyrus; STG = superior temporal gyrus; INS = insular cortex.

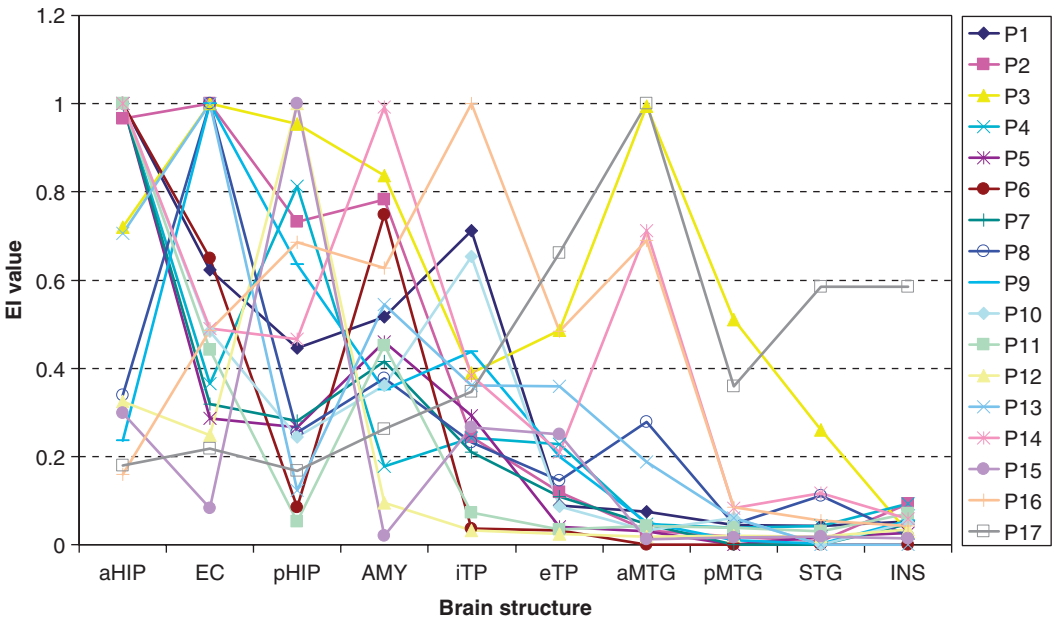

Fig. 5 Individual profiles of epileptogenicity. EI values are plotted for each patient and for each studied structure.

made about this figure. First, all mesial structures (black colour) disclose higher mean EI values than lateral structures (grey colour). Secondly, among the mesial structures, the highest mean EI values were obtained from the anterior hippocampus and the EC. However, although these two structures have been recognized to play an important role in MTLE, there is no 'clear-cut' distinction between them and the three other internal structures of the temporal lobe (pHIP, AMY and iTP). Indeed, the observed gradient of EI values suggests that the EZ cannot be reduced to a unique structure but rather corresponds to a more complex network that extends over brain areas with gradual epileptogenicity.

Inter-individual variability

In the previous section, mean EI values were analysed according to the mesial or lateral location of considered structures in the temporal region. In order to consider patient-specific features, EI values were plotted for each patient and for each structure, as displayed in Fig. 5. Visual inspection of the obtained curves showed that the 'patterns of epileptogenicity' could considerably vary from one patient to the other. The EC was found to be the more epileptogenic structure in P2, P3, P8, P9, P13 as was the anterior hippocampus (aHIP) in patients P1, P4, P5, P6, P7, P10, P11 and P14. The posterior hippocampus (pHIP) had the highest EI values in P3, P12 and P15.

It is noteworthy that some structures were found to have low EI values in the majority of patients. These included the insular region (INS), the posterior temporal neocortex (pMTG) and the superior temporal gyrus (STG). Figure 5 also shows the already-mentioned different profile of patient 17 (P17) who had higher values in the temporal neocortex than in the other structures.

Relationship with HS

We further examined the possibility that involved networks could differ according to the underlying pathology (Fig. 6). Moderate to marked HS was observed in 13 patients and normal MRI (without HS) in 4 patients. In the group of patients with normal MRI (P3, P14, P16, P17), EI values computed from the lateral temporal pole (eTP, $P = 0.009$), the middle temporal gyrus (aMTG $P = 0.003$, pMTG $P = 0.003$) and the superior temporal gyrus (STG, $P = 0.004$) were significantly higher than the EI values obtained from similar structures in the group of patients with HS (P1, P2, P4–P13, P15). Consequently, these results strongly suggest that epileptogenic networks in patients with normal MRI not only include the mesial structures but also extend beyond the limbic system, in particular to the lateral neocortex. We investigated this hypothesis in more detail by computing, in both groups of patients, the number of structures disclosing a high epileptogenicity index (EI value >0.3, see Fig. 4), assuming that a high number would reflect more extended epileptogenic zone.

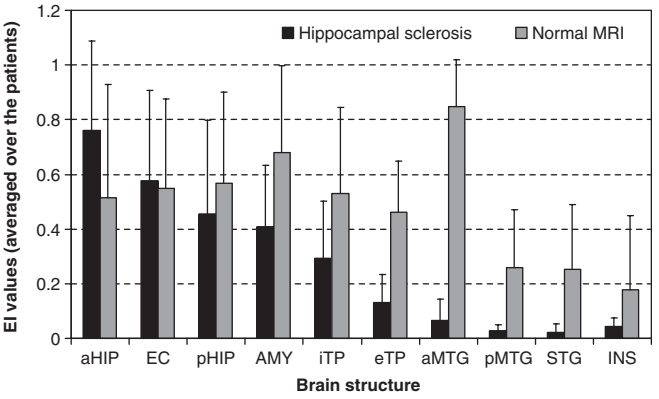

Fig. 6 Mean EI values and standard deviations measured from recorded structures in patients with hippocampal sclerosis (black) or with normal MRI (grey).

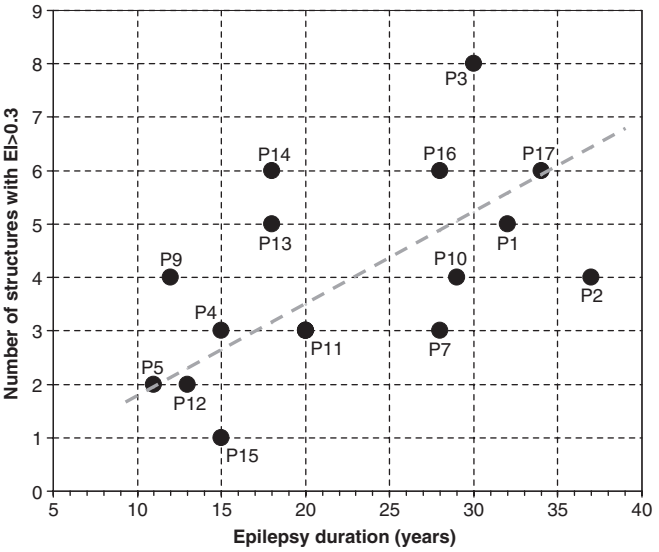

Fig. 7 Relationship between the number of structures disclosing an EI value greater than 0.3 ($N_{IE \geqslant 0.3}$) and the duration of epilepsy in the 17 studied patients.

This number, denoted by $N_{IE \geqslant 0.3}$, was found to be different in the normal MRI group ($N_{IE \geqslant 0.3} = 5.7 \pm 0.5$) and in the HS group ($N_{IE \geqslant 0.3} = 3.1 \pm 1.2$).The difference reached a significant level ($P = 0.004$, Mann–Whitney test) and confirmed that the epileptogenicity in the normal MRI group is spatially more extended than in the HS group.

Relationship between epileptogenicity of the temporal lobe and epilepsy duration

We also studied the assumption according to which the extension of epileptogenic networks might be correlated with the duration of the epilepsy. To proceed, we looked for statistical correlations between EI values and the epilepsy duration. Neither the mean IE values computed from mesial (Spearman $P = 0.16$) nor from lateral (Spearman $P = 0.21$) structures were correlated with the epilepsy duration. Conversely, we found a statistically

significant ($P = 0.01$) linear correlation between the number of structures disclosing a high epileptogenicity index (i.e. IE $\geqslant 0.3$) and the duration of the epilepsy. This relation is shown in Fig. 7. As depicted, the number of structures exhibiting an EI larger than 0.3 increases with epilepsy duration. No correlation between age at the onset of the disease and the number of high EI values was found ($P = 0.75$). These results suggest that MTLE is a gradually evolving process in which the epileptogenicity of the temporal lobe tends to increase with time.

Relationship with surgical outcome

The relationship between epileptogenicity and surgical outcome is a crucial issue that is difficult to definitively assess in a limited series of patients. Indeed most of these patients had an anterior temporal lobectomy tailored according to the result of SEEG. This procedure led to a favourable outcome in most of the patients. As indicated in Table 1, most of the epileptogenic structures were removed by the procedure. We observed a trend for a better outcome in patients with less epileptogenic structures since patients with the better surgical outcome (IA) have a mean of 3.1 $N_{IE \geqslant 0.3}$ and patients not in Engel class IA a mean of 4.5 ($P = 0.1$). We expect that this result will be further confirmed by a study on a larger population including extra-temporal lobe epilepsies.

Discussion

This study constitutes an attempt to define the organization of the epileptogenic zone (EZ) from a quantitative measure that characterizes the epileptogenicity of brain structures explored with depth electrodes. The EZ was defined here in its historical definition (Bancaud *et al.*, 1965), corresponding to the 'ictal onset zone' of other groups (Rosenow and Luders, 2001).

This measure, called 'Epileptogenicity Index' (EI), is based on both spectral (appearance of high-frequency oscillations replacing the background activity) and temporal (delay of appearance with respect to seizure onset) properties of intracerebral EEG signals recorded during presurgical evaluation.

The main findings of this study were as follows:

(a) In the studied group of patients with MTLE, EI values computed from mesial structures of the temporal lobe were found to be higher than values computed from structures not involved at seizure onset. This result validates the proposed approach, showing that a quantification of the 'epileptogenicity' can be obtained from depth-EEG signals.

(b) In the majority of patients, significantly high EI values were computed in more than one structure of the temporal lobe region. In addition, when averaged over patients, the degree of epileptogenicity gradually decreased from structure to structure. These results show that the EZ most often organizes as an extended network that can hardly be reduced to a single 'focus'.

(c) In patients with normal MRI compared with patients with HS, higher EI values were found for lateral neocortex and a greater number of epileptogenic structures were found. This shows that the pattern of epileptogenicity can differ with respect to the underlying pathology.

(d) A statistically significant correlation was found between the duration of epilepsy and the number of structures disclosing high epileptogenicity.

These four points are discussed in the following.

Quantification of 'epileptogenicity' from intracerebral EEG signals

Our primary intent was to quantify the 'epileptogenicity' of a given brain structure from the field potentials it generates during the seizure period. The proposed quantity is based on a typical electrophysiological pattern, also referred to as the 'rapid discharge' or 'high frequency epileptiform oscillations' (Worrell *et al.*, 2004; Jirsch *et al.*, 2006). This pattern was initially described by Bancaud *et al.* (1965). It is now recognized as a characteristic marker of the onset of focal seizures, provided that electrodes are appropriately positioned in target sites. The spectral properties of rapid discharges observed at seizure onset were quantified in several studies (Allen *et al.*, 1992; Alarcon *et al.*, 1995; Wendling *et al.*, 2003; Worrell *et al.*, 2004; Jirsch *et al.*, 2006).

In this study, we go beyond the description of the frequency content of signals. Using assumptions based on a long practice of intracerebral EEG, we have proposed an index that makes use of (i) the signal energy in well-defined frequency bands (appearance of beta–gamma oscillations concomitantly with the attenuation of slower alpha–theta oscillations) and (ii) the time at which rapid discharges occur. The combination of these two factors in a single quantity provides a good characterization of the epileptogenicity of explored brain structures: the absence (resp. presence) of a rapid discharge and/or the late (resp. early) involvement in the seizure process contributes to low (resp. high) EI value. It is noteworthy that several experimental (Traub *et al.*, 2001) and computational modelling (Wendling *et al.*, 2005) studies also demonstrated the existence of a relationship between the epileptogenicity of the neuronal tissue and its propensity to generate fast oscillations.

From the methodological view point, the well-known difficult problem of detection of changes in non-stationary signals had to be solved in order to automatically estimate the EI value. As in any detection problem, some parameters must be adjusted to control the sensitivity and the specificity of the method. In the algorithm we implemented, two parameters (threshold and bias) must be set in order to detect the onset of the rapid discharge. Although the algorithm was found to perform well in most situations, we decided to implement a semi-automatic approach, at this

stage. These two parameters are interactively adjusted under visual control and once the operator agrees on the detection time provided by the algorithm, then the EI value is computed. Future work will deal with the comparison of reported results with those obtained from a fully automatic method.

The association between signal frequency content and latency of fast oscillations in a quantitative index is a specific feature which makes the proposed method different from synchrony-based methods used to characterize signal changes occurring during the transition from interictal to ictal activity. For instance, in an experimental model (*in vitro* preparation), the sliding covariance- and correlation-based indices proposed in (Cohen *et al.*, 2006) permitted to quantify the coherence of spike trains generated by cell populations located in different sites in an during disinhibition (induced by GABA receptor antagonist). In humans, numerous studies also reported methods aimed at estimating interdependencies between depth-EEG signals. In particular, results obtained from non-linear correlation-based (Pijn and Lopes Da Silva, 1993; Wendling *et al.*, 2001) or coherence-based (Lieb *et al.*, 1987; Gotman and Levtova, 1996) methods have shown that preferential interactions occur between mesial temporal lobe structures in temporal lobe seizures. The aforementioned methods provide different—and possibly complementary—information about the epileptogenic zone, with respect to the method described in this paper. Therefore, a question, which is beyond the scope of this study, is raised: what is the relationship between the sites showing larger 'epileptogenicity index' and those showing altered synchronization degree?

Network organization of the epileptogenic zone in MTLE

In patients included in this study, the EZ was located in the mesial region of the temporal lobe. Interestingly, highest values of the EI indicated that the EZ was not restricted to a single mesial structure (i.e. a 'focus'), but rather corresponded to a set of mesial structures, mostly in the anterior part of the temporal region. This result is in line with the view that extended networks are affected in MTLEs. Such networks may include not only the hippocampus but also the sub-hippocampal structures such as the EC and the limbic part of the temporal pole (Suzuki and Amaral, 2003). This is in accordance with previous reports based on electrophysiological recordings or neuroanatomical studies pointing out the role of structures other than the hippocampus in the pathophysiology of mesial temporal lobe epilepsies (Spencer and Spencer, 1994; Bernasconi *et al.*, 2000, 2001; Velasco *et al.*, 2000; Bartolomei *et al.*, 2001*b*; Briellmann *et al.*, 2004).

Results are important to consider for surgical approaches, particularly when selective procedures are chosen. Failure of selective amygdalo-hippocampectomy (Yasargil *et al.*, 1993) or radiosurgery gamma knife (Regis *et al.*, 2000) could be related to the wide epileptogenicity observed in some patients, particularly extension to the temporal pole (Chabardes *et al.*, 1999) or to the posterior hippocampus (Baulac *et al.*, 1994). Even if MTLE associated with HS is considered to be a relatively homogeneous entity, individual results clearly show variable epileptogenicity profiles from one patient to the other. However, taken as a whole, our results indicate that the two most epileptogenic structures in MTLE-HS are the anterior hippocampus and the EC, corroborating the good results observed after surgical removal (Goldring *et al.*, 1992) or radiosurgical targetting (Regis *et al.*, 2000) of these two structures.

Epileptogenicity, normal MRI and HS

Our results show that the neocortex is more epileptogenic in patients with normal MRI, compared to patients with HS. The number of epileptogenic structures was also higher in this subgroup of MTLE patients. These results suggest that the organization of the EZ is different in these two subgroups of patients diagnosed with MTLE, with a 'wider' epileptogenic network extending beyond the mesial structures in the former subgroup. Interestingly, some recent studies revealed that this group of patients could be characterized by different histological and neurophysiological features (Cohen-Gadol *et al.*, 2005) and also by a poorer seizure outcome after surgery (Garcia *et al.*, 1994; Zaveri *et al.*, 2001; Sylaja *et al.*, 2004; Janszky *et al.*, 2005; Cohen-Gadol *et al.*, 2005; Araujo *et al.*, 2006). We suspect that the more extended epileptogenic networks we found in patients with normal MRI could be the reason for surgical failure, as has also been previously suggested (Cohen-Gadol *et al.*, 2005). Conversely, the higher rate of surgery success in patient with HS could be explained by the fact that epileptogenic networks remain more confined within mesial structures.

Relationship between the extension of the epileptogenic zone and the duration of epilepsy

It has long been proposed that epileptogenesis is an active process that could develop over years. Some studies have reported a significant relationship between the epilepsy duration and the degree of mesial temporal atrophy (Bernasconi *et al.*, 2005; Liu *et al.*, 2005). A long period between onset of epilepsy and eventual epilepsy surgery is therefore often considered to be a poor prognostic factor, as reported in studies evaluating seizure outcome following anterior temporal lobectomy [review in (McIntosh *et al.*, 2001)].

We found that the extent of the EZ, as characterized by the number of structures disclosing high EI values, is strongly correlated with the duration of epilepsy. This finding may be interpreted as the gradually increasing propensity of epileptogenic networks to generate rapid discharges. This interpretation also relates to the so-called

secondary epileptogenesis process. According to this mechanism, well demonstrated in animal models, the recurrence of epileptic discharges taking place in one structure of the network are able to induce neurobiological changes in the other structures of the network. On the long term, these changes lead to epileptic discharges in the other structures and provoke an extension of epileptogenic networks (Morrell, 1989; Sutula, 2001; Wilder, 2001). Our findings add strong arguments for the existence of such mechanisms in human epilepsy and suggest that early surgery may be potentially more efficient in patients with drug-resistant epilepsy.

Conclusion

The determination of the epileptogenicity of brain regions potentially involved in seizure generation is crucial in the context of epilepsy surgery. Our study in a selected population of patients with TLE has shown that the proposed index (EI) may give important indication about regions affected by the epileptogenic process and about its spatial extent. This determination may be useful in clinical practice as well as in the research field. Quantification of the EZ may be the basis for precise depth-surface comparison or for metabolic studies in drug-resistant epilepsies. It may also be an additional help for the clinician to precisely determine the region of the brain to be removed. Future studies will evaluate this method in other types of partial epilepsies and the relationship with surgical prognosis in a larger cohort of patients.

Acknowledgements

We thank Dr M Gavaret, Dr M Guye, Dr A Trébuchon, Dr A McGonigal (Department of Clinical Neurophysiology, Marseille) for clinical and electrophysiological assessment of studied patients. We thank Prof. J. Régis (Neurosurgery Department, Marseille) for the stereotactic placement of electrodes.

References

Alarcon G, Binnie CD, Elwes RD, Polkey CE. Power spectrum and intracranial EEG patterns at seizure onset in partial epilepsy. Electroencephalogr Clin Neurophysiol 1995; 94: 326–37.

Allen PJ, Fish DR, Smith SJ. Very high-frequency rhythmic activity during SEEG suppression in frontal lobe epilepsy. Electroencephalogr Clin Neurophysiol 1992; 82: 155–9.

Araujo D, Santos AC, Velasco TR, Wichert-Ana L, Terra-Bustamante VC, Alexandre V Jr, et al. Volumetric evidence of bilateral damage in unilateral mesial temporal lobe epilepsy. Epilepsia 2006; 47: 1354–9.

Bancaud J, Angelergues R, Bernouilli C, Bonis A, Bordas-Ferrer M, Bresson M, et al. Functional stereotaxic exploration (SEEG) of epilepsy. Electroencephalogr Clin Neurophysiol 1970; 28: 85–6.

Bancaud J, Talairach J, Bonis A, Schaub C, Szikla G, Morel P, et al. La stéréoélectroencéphalographie dans l'épilepsie: informations neurophysiopathologiques apportées par l'investigation fonctionnelle stereotaxique. Paris: Masson; 1965.

Bartolomei F, Barbeau E, Gavaret M, Guye M, McGonigal A, Regis J, et al. Cortical stimulation study of the role of rhinal cortex in deja vu and reminiscence of memories. Neurology 2004a; 63: 858–64.

Bartolomei F, Khalil M, Wendling F, Sontheimer A, Regis J, Ranjeva JP, et al. Entorhinal cortex involvement in human mesial temporal lobe epilepsy: an electrophysiologic and volumetric study. Epilepsia 2005; 46: 677–87.

Bartolomei F, Wendling F, Bellanger J, Regis J, Chauvel P. Neural networks involved in temporal lobe seizures: a nonlinear regression analysis of SEEG signals interdependencies. Clin Neurophysiol 2001a; 112: 1746–60.

Bartolomei F, Wendling F, Bellanger JJ, Regis J, Chauvel P. Neural networks involving the medial temporal structures in temporal lobe epilepsy. Clin Neurophysiol 2001b; 112: 1746–60.

Bartolomei F, Wendling F, Regis J, Gavaret M, Guye M, Chauvel P. Pre-ictal synchronicity in limbic networks of mesial temporal lobe epilepsy. Epilepsy Res 2004b; 61: 89–104.

Basseville M, Nikiforov I. Detection of abrupt changes: theory and application. Information and system science series. Englewood Cliffs, NJ: Prentice-Hall, Inc; 1993.

Baulac M, Saint-Hilaire JM, Adam C, Martinez M, Fontaine S, Laplane D. Correlations between magnetic resonance imaging-based hippocampal sclerosis and depth electrode investigation in epilepsy of the mesio-temporal lobe. Epilepsia 1994; 35: 1045–53.

Bernasconi N, Bernasconi A, Caramanos Z, Andermann F, Dubeau F, Arnold DL. Morphometric MRI analysis of the parahippocampal region in temporal lobe epilepsy. Ann NY Acad Sci 2000; 911: 495–500.

Bernasconi N, Bernasconi A, Caramanos Z, Dubeau F, Richardson J, Andermann F, et al. Entorhinal cortex atrophy in epilepsy patients exhibiting normal hippocampal volumes. Neurology 2001; 56: 1335–9.

Bernasconi N, Natsume J, Bernasconi A. Progression in temporal lobe epilepsy: differential atrophy in mesial temporal structures. Neurology 2005; 65: 223–8.

Bragin A, Wilson CL, Engel J Jr. Chronic epileptogenesis requires development of a network of pathologically interconnected neuron clusters: a hypothesis. Epilepsia 2000; 41 (Suppl 6): S144–52.

Briellmann RS, Jackson GD, Pell GS, Mitchell LA, Abbott DF. Structural abnormalities remote from the seizure focus: a study using T2 relaxometry at 3 T. Neurology 2004; 63: 2303–8.

Chabardes S, Kahane P, Hoffman D, Munari C, Benabid AL. Role of the temporo-polar region in the genesis of temporal lobe seizures. Epilepsia 1999; 40 (Suppl 7): 78.

Cohen I, Huberfeld G, Miles R. Emergence of disinhibition-induced synchrony in the CA3 region of the guinea pig hippocampus in vitro. J Physiol 2006; 570: 583–94.

Cohen-Gadol AA, Bradley CC, Williamson A, Kim JH, Westerveld M, Duckrow RB, et al. Normal magnetic resonance imaging and medial temporal lobe epilepsy: the clinical syndrome of paradoxical temporal lobe epilepsy. J Neurosurg 2005; 102: 902–9.

Garcia PA, Laxer KD, Barbaro NM, Dillon WP. Prognostic value of qualitative magnetic resonance imaging hippocampal abnormalities in patients undergoing temporal lobectomy for medically refractory seizures. Epilepsia 1994; 35: 520–4.

Goldring S, Edwards I, Harding G, Bernardo K. Results of anterior temporal lobectomy that spares the amygdala in patients with complex partial seizures. J Neurosurg 1992; 77: 185–93.

Gotman J, Levtova V. Amygdala-hippocampus relationships in temporal lobe seizures: a phase coherence study. Epilepsy Res 1996; 25: 51–7.

Hinkley D. Inference about the change point from cumulative sum-tests. Biometrika 1970; 58: 509–23.

Janszky J, Pannek HW, Janszky I, Schulz R, Behne F, Hoppe M, et al. Failed surgery for temporal lobe epilepsy: predictors of long-term seizure-free course. Epilepsy Res 2005; 64: 35–44.

Jirsch JD, Urrestarazu E, LeVan P, Olivier A, Dubeau F, Gotman J. High-frequency oscillations during human focal seizures. Brain 2006; 129: 1593–608.

Lieb J, Hoque K, Skomer C, Song X. Interhemispheric propagation of human medial temporal lobe seizures: a coherence/phase analysis. Electroencephal Clin Neurophysiol 1987; 67: 101–19.

Liu RS, Lemieux L, Bell GS, Sisodiya SM, Bartlett PA, Shorvon SD, et al. Cerebral damage in epilepsy: a population-based longitudinal quantitative MRI study. Epilepsia 2005; 46: 1482–94.

Maillard L, Vignal JP, Gavaret M, Guye M, Biraben A, McGonigal A, et al. Semiologic and electrophysiologic correlations in temporal lobe seizure subtypes. Epilepsia 2004; 45: 1590–9.

Mangin JF, Riviere D, Cachia A, Duchesnay E, Cointepas Y, Papadopoulos-Orfanos D, et al. A framework to study the cortical folding patterns. Neuroimage 2004; 23 (Suppl 1): S129–38.

McIntosh AM, Wilson SJ, Berkovic SF. Seizure outcome after temporal lobectomy: current research practice and findings. Epilepsia 2001; 42: 1288–307.

Morrell F. Varieties of human secondary epileptogenesis. J Clin Neurophysiol 1989; 6: 227–75.

Niedermeyer E, Lopes Da Silva F. Electroencephalography: basic principles, clinical applications, and related fields. 4th edn. Baltimore: Williams & Wilkins; 1999.

Page E. Continuous inspection schemes. Biometrika 1954; 41: 100–15.

Pijn J, Lopes Da Silva F. Propagation of electrical activity: nonlinear associations and time delays between EEG signals. In: Zschocke St. and Speckmann EJ, editors. Basic mechanisms of the EEG. Boston: Birkauser; 1993.

Regis J, Bartolomei F, Hayashi M, Roberts D, Chauvel P, Peragut JC. The role of gamma knife surgery in the treatment of severe epilepsies. Epileptic Disord 2000; 2: 113–22.

Regis J, Mangin JF, Ochiai T, Frouin V, Riviere D, Cachia A, et al. ''Sulcal root'' generic model: a hypothesis to overcome the variability of the human cortex folding patterns. Neurol Med Chir 2005; 45: 1–17.

Rosenow F, Luders H. Presurgical evaluation of epilepsy. Brain 2001; 124: 1683–700.

Spencer S, Guimaraes P, Katz A, Kim J, Spencer D. Morphological patterns of seizures recorded intracranially. Epilepsia 1992; 33: 537–45.

Spencer S, Spencer D. Entorhinal-hippocampal interactions in medial temporal lobe epilepsy. Epilepsia 1994; 35: 721–7.

Spencer SS. Neural networks in human epilepsy: evidence of and implications for treatment. Epilepsia 2002; 43: 219–27.

Sutula TP. Secondary epileptogenesis, kindling, and intractable epilepsy: a reappraisal from the perspective of neural plasticity. Int Rev Neurobiol 2001; 45: 355–86.

Suzuki WA, Amaral DG. Perirhinal and parahippocampal cortices of the macaque monkey: cytoarchitectonic and chemoarchitectonic organization. J Comp Neurol 2003; 463: 67–91.

Sylaja PN, Radhakrishnan K, Kesavadas C, Sarma PS. Seizure outcome after anterior temporal lobectomy and its predictors in patients with apparent temporal lobe epilepsy and normal MRI. Epilepsia 2004; 45: 803–8.

Talairach J, Bancaud J, Bonis A, Szikla G, Trottier S, Vignal JP, et al. Surgical therapy for frontal epilepsies. Adv Neurol 1992; 57: 707–32.

Traub RD, Whittington MA, Buhl EH, LeBeau FE, Bibbig A, Boyd S, et al. A possible role for gap junctions in generation of very fast EEG oscillations preceding the onset of, and perhaps initiating, seizures. Epilepsia 2001; 42: 153–70.

Velasco A, Wilson C, Babb T, Engel J. Functional and anatomic correlates of two frequently observed temporal lobe seizure-onset patterns. Neural Plasticity 2000; 7: 49–63.

Wendling F, Bartolomei F, Bellanger J, Chauvel P. Interpretation of interdependencies in epileptic signals using a macroscopic physiological model of EEG. Clin Neurophysiol 2001; 112: 1201–18.

Wendling F, Bartolomei F, Bellanger JJ, Bourien J, Chauvel P. Epileptic fast intracerebral EEG activity: evidence for spatial decorrelation at seizure onset. Brain 2003; 126: 1449–59.

Wendling F, Hernandez A, Bellanger J, Chauvel P, Bartolomei F. Interictal to ictal transition in human temporal lobe epilepsy: insights from a computational model of intracerebral EEG. J Clin Neurophysiol 2005; 22: 343–56.

Wieser H. Electroclinical features of the psychomotor seizures. London, England: Butterworths; 1983.

Wilder BJ. The mirror focus and secondary epileptogenesis. Int Rev Neurobiol 2001; 45: 435–46.

Worrell GA, Parish L, Cranstoun SD, Jonas R, Baltuch G, Litt B. High-frequency oscillations and seizure generation in neocortical epilepsy. Brain 2004; 127: 1496–506.

Yasargil M, Wieser H, Valanis A, von Ammon K, Roth P. Surgery and results of the selective amygdala-hippocampectomy in one hundred patients with nonlesional limbic epilepsy. Neurosurg Clin N Am 1993; 4: 243–61.

Zaveri HP, Duckrow RB, de Lanerolle NC, Spencer SS. Distinguishing subtypes of temporal lobe epilepsy with background hippocampal activity. Epilepsia 2001; 42: 725–30.